infrastructures

MDPI

Article

Evaluation of the Bond-to-Concrete Properties of GFRP Rebars in Marine Environments

Alvaro Ruiz Emparanza [1,*]**, Francisco De Caso Y Basalo** [1]**, Raphael Kampmann** [2] **and Itziar Adarraga Usabiaga** [3]

[1] Department of Civil, Architectural and Environmental Engineering, University of Miami, Coral Gables, FL 33146, USA; fdecaso@miami.edu

[2] Department of Civil and Environmental Engineering, Florida State University, Tallahassee, FL 32310, USA; kampmann@eng.famu.fsu.edu

[3] Department of Mechanical Engineering, University of the Basque Country, 20018 San Sebastian, Guipuzcoa, Spain; itziar.adarraga@ehu.eus

* Correspondence: axr1489@miami.edu; Tel.: +1-850-800-7904

check for updates

Abstract: Increased traffic in combination with growing environmental impacts have led to the accelerated degradation of built infrastructure. In reinforced concrete structures, the corrosion of steel reinforcement is the predominant cause of deterioration. Thus, over the last years the use of glass fiber reinforced polymer (GFRP) composites as internal reinforcement bars (rebars) for concrete structures has been evaluated, and has been proved to be a viable alternative to traditional steel reinforcement mainly due to its tensile strength and non-corrosive nature. However, thus far, the GFRP rebar market is diverse and manufacturers around the world produce GFRP rebar types with different surface enhancements to improve the bond to concrete characteristics. In this study, the bond performance of three dissimilar GFRP rebar types (sand coated, helically grooved and with surface lugs) was evaluated over time in seawater environments, with a focus on the bond strength. Accordingly, specimens were exposed to seawater in circulating chambers at three different temperatures (23 °C, 40 °C and 60 °C) for multiple time periods (60 and 120 days). To evaluate the bond performance, pullout tests were conducted according to ASTM D7913. The results showed that the bond strength varied with the surface enhancement features. However, the bond strength did not vary significantly with exposure time and temperature for all three evaluated rebar types.

1. Introduction

Within the last three decades, glass fiber reinforced polymer (GFRP) rebars have been successfully used as an alternative to traditional steel reinforcement for internally reinforced concrete structures [1] due to their superior properties, specifically the resistance to corrosion. Accordingly, the Florida Department of Transportation (FDOT) and other North American institutions are investing in the development of this alternative technology for its use in coastal applications, where corrosion is one of the main deteriorating mechanisms [2–5]. In addition to corrosion resistance, GFRP rebars offer high tensile strength (2–3 times higher than steel rebars of equal diameter), are lightweight (1/4 of the weight of steel), and they are transparent to magnetic fields [6].

GFRP rebars are composite elements made from longitudinal glass fibers embedded in a resin matrix—most commonly vinyl ester or epoxy—which are manufactured via 'pultrusion' methods. One of the major concerns for the full development of this technology is the lack of standardization; today, the GFRP rebar market is diverse because different producers manufacture rebars with different

raw materials (fibers and resin), different cross-sections (round, oval, quadratic, etc.), and different surface enhancements (sand coating, helical wrap, lugs, etc.) [1]. The latter are responsible for the quality/enhancement of the bond between the GFRP rebars and concrete, ensuring the composite action of both materials. To transfer the stresses from the concrete to the rebar, a proper bond is crucial. The bond mechanism is governed by the mechanical interaction, chemical adhesion, and frictional forces between the GFRP rebar and the concrete. In addition, it depends on the nominal diameter of the rebars, surface enhancement, concrete cover, bond length, and concrete strength [7].

The bond capacity of GFRP rebars, for acceptance criteria purposes, is most commonly evaluated through the 'pullout-test' method as per ASTM D7913 [8]. In design, the coefficient that reflects the bond behavior of the different rebar types is the k_b or bond factor [7]. Thus far in North America, this factor is obtained via four-point-bending tests described in CSA S806-12 [9] Annex-S.

Although many researchers have analyzed the bond behavior of different rebars in the past years [10], only a few studies have addressed the durability of this mechanical property. The long-term performance of a proper stress transfer between GFRP rebars and concrete throughout the life-span of a GFRP reinforced concrete structure is the critical aspect that ultimately defines the quality of the bond. Researchers such as Amad Altalmas et al. or Zhiqiang Dong et al. [11,12] studied the bond durability of basalt FRP rebars (BFRP) exposed to alkaline and seawater solutions, while Mathieu Robert et al. [13] examined the bond durability of GFRP rebars exposed to tap water. However, the durability of GFRP rebars exposed to seawater has not been fully assessed, neither wholly evaluated by code writing authorities. For example, the Florida Department of Transportation (FDOT) does not yet allow the use of GFRP rebars in water-submerged concrete elements.

2. Problem Statement and Research Significance

In civil engineering, the resilience of the built infrastructure is crucial and has to be ensured throughout a service life period defined by applicable design codes. For GFRP reinforced concrete structures, different studies have separately verified the durability of concrete and GFRP reinforcement [2–5,14]. However, additional research is needed to determine the time-dependent degradation of the interface between both elements in aggressive environments, such as saltwater.

The purpose of this research work is to analyze and characterize the bond behavior of three different GFRP rebar types (with their respective surface enhancement) and to quantify the degradation of this mechanical property in response to harsh saltwater environments found in coastal areas. The results will provide deeper insight into this mechanical property and help future researchers to optimize design coefficients such as the bond factor (k_b) or the environmental factor (C_E), while taking the durability of the bond into account. This will lead to a more efficient design of reinforced concrete structures with non-corrosive reinforcement.

3. Materials and Methods

In this research project, the bond behavior of three commercial GFRP rebars was studied. To evaluate the bond behavior, the pull-out method proposed by the American Society for Testing and Materials, ASTM D7913 [8], was used.

3.1. Materials

Before the bond tests were conducted, both the concrete and the GFRP bars were characterized individually for bench mark values and quality control. Likewise, these values were used to characterize the overall bond performance.

3.1.1. Concrete

The pullout specimens were made from the structural concrete that the Florida Department of Transportation (FDOT) requires for the construction of bridge decks in Florida, USA. This concrete, known as 'Classe II 4500 Bridgedeck', has a guaranteed compressive strength of 4500 psi (31.03 MPa).

To obtain the compressive strength of the concrete, companion specimens were tested according to ASTM C39 [15]. At different maturity levels (3 d, 7 d, 14 d and 28 d after the concrete was cast), five cylindrical concrete specimens were evaluated, resulting a compressive strength at 28 days of 37.20 MPa with a standard deviation of 0.67 MPa (coefficient of variation of 1.8%).

3.1.2. GFRP Rebars

Three types of commercially available rebars were used, all with a nominal diameter of 10 mm and different surface enhancements (see Figure 1).
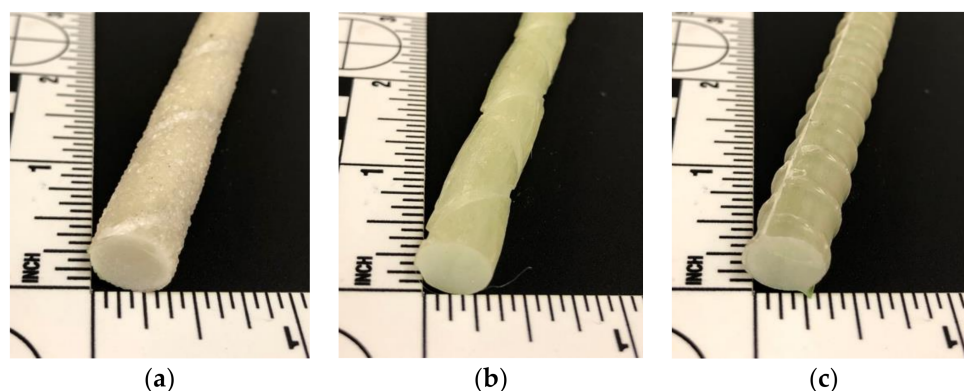

| (a) | (b) | (c) |

Figure 1. GFRP rebar type A (**a**), type B (**b**) and type C (**c**).

These bars were characterized in the materials and structures laboratory at the University of Miami and the FAMU-FSU College of Engineering. The obtained values are summarized in Table 1.

Table 1. Properties of the GFRP rebars.

Rebar Type	Nominal Diameter	Measured Diameter	Surface Enhancement	Tensile Strength	Elastic Modulus
	mm	mm		MPa	GPa
A		10.17	Sand coating	826.00	45.37
B	10 mm	10.45	Helical wrap	550.20	50.68
C		9.58	Lugs	804.62	51.37

The actual diameters were measured according to ASTM D792 [16], while the guaranteed maximum tensile strengths and the modulus of elasticity were measured per ASTM D7205 [17].

3.2. Specimen Preparation

In total, 63 specimens were prepared for the 'pullout' test procedure as described in ASTM D7913 [8]. The loaded end of the rebar (the end where the load was applied) was protected with a 300 mm long steel pipe to shield the rebar from the grips. This was necessary due to the low transverse strength of the FRP rebars. The other end of the rebar, however, was embedded in a 200 × 200 × 200 mm concrete cube. To break the bond between the rebar and the concrete, 150 mm of the rebar (inside the cubes) were shielded to guarantee a pure bond length of five times the diameter (50 mm in this case). The specimens were cast using individual plywood molds, where fresh concrete was placed in two layers (each layer was equally compacted with an internal vibrator). The specimens were demolded after two days, and left to cure under ambient conditions for 28 days before the specimens were tested or exposed to the aging environment.

3.3. Aging Conditioning Protocol

To accelerate the deterioration of the bond between the GFRP rebars and the concrete, the specimens were exposed to seawater at different temperatures. Of the 63 specimens, 54 were submerged in seawater tanks (see Figure 2), while the remaining nine were tested in their virgin state without conditioning, to obtain control values for the analysis of the potential deterioration (see Table 2).
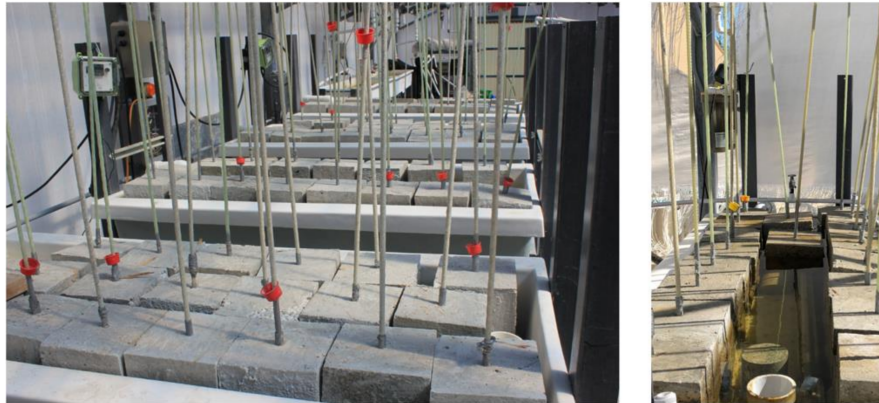

Figure 2. Conditioning exposure of the specimens.

Table 2. Experimental maximum values of the bond between the GFRP rebars and the concrete.

Rebar Type	Exposure Time	Temperature	'Pull-Out' Load (Average)		Bond Strength (Average)	
			kN	kip	MPa	ksi
A	cc	cc [1]	29.37	6.60	18.39	2.67
	60 d	23	23.54	5.29	14.73	2.14
		40	29.46	6.62	18.44	2.68
		60	26.03	5.85	16.29	2.36
	120 d	23	25.04	5.63	15.68	2.27
		40	23.46	5.27	14.68	2.13
		60	25.32	5.69	15.85	2.30
B	cc	cc [1]	30.77	6.92	18.75	2.72
	60 d	23	26.70	6.00	16.26	2.36
		40	27.64	6.21	16.84	2.44
		60	29.82	6.70	18.17	2.64
	120 d	23	32.67	7.35	19.90	2.89
		40	32.22	7.24	19.63	2.85
		60	28.15	6.33	17.15	2.49
C	cc	cc [1]	33.52	7.54	22.28	3.23
	60 d	23	28.01	6.30	18.62	2.70
		40	31.16	7.01	20.71	3.00
		60	30.98	6.97	20.59	2.99
	120 d	23	31.92	7.18	21.21	3.08
		40	29.61	6.66	19.68	2.85
		60	30.00	6.74	19.93	2.89

[1] control values (non-aged specimens).

The specimens were exposed to three different environments: of the 54 specimens that were submerged in seawater, 18 were exposed to 23 ° C, 18 to 40 °C and the last 18 to 60 °C. Each group of 18 rebars was formed by six rebars of each type (A, B and C). The reasons these temperatures were chosen included: (i) 23C for laboratory conditions; (ii) 60C because it is most commonly used in

accelerated conditioning protocols for FRP rebars [3,18] and because it is proposed by ASTM D7705 [19] for the aging of GFRP rebars in alkaline water; and (iii) 40C for reference values in between.

3.4. Test and Instrumentation

The specimens were tested following the method proposed in ASTM D7913 [8]. The tests were conducted in displacement control mode in a universal test frame with a capacity of 890 kN. The load-displacement development throughout the test was monitored and the bond behavior after the maximum load was reached ('post-failure' behavior) was recorded. The load was applied through a displacement rate of 0.5 mm/min. The applied load was recorded by the load cell integral to the test frame, while the displacement was recorded using three displacement transducers or LVDTs: two of them were placed on the loaded end of the rebar, while the third one was placed on the lower part of the concrete cube or free end of the rebar, as can be seen in Figure 3.
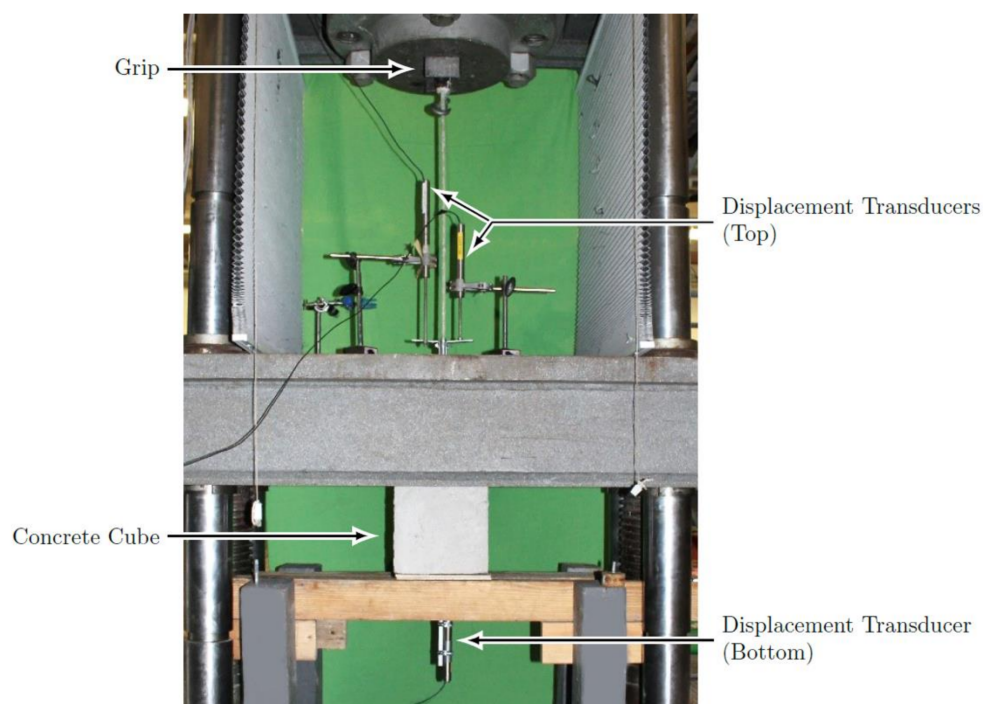

Figure 3. 'Pull-out' test setup.

The data for both parameters (load and displacement) was recorded using an automatic data acquisition system with a data rate of 10 Hz. The results were filtered using the Butterworth methods.

4. Results and Discussion

The experimental results obtained from the 63 specimens tested were analyzed following the specifications defined in ASTM D7913 [8]. The bond strength was computed using the following Equation (1):

$$\tau = F/(C_d \cdot l), \tag{1}$$

where 'τ' is the average bond strength (MPa), 'F' is the maximum applied load (N), 'l' is the bond length (mm) and 'C_d' is the effective circumference, $\pi \cdot d_b$ (mm).

Prior to the analysis of the aged bond properties of the GFRP rebars, the bond behavior of unaged bond specimens was evaluated. Figure 4 shows the bond strength vs. free-end slippage of each of the tested unaged composite rebars. For each rebar type, the envelope including the bond-slip behavior of the three tested specimens is shown.
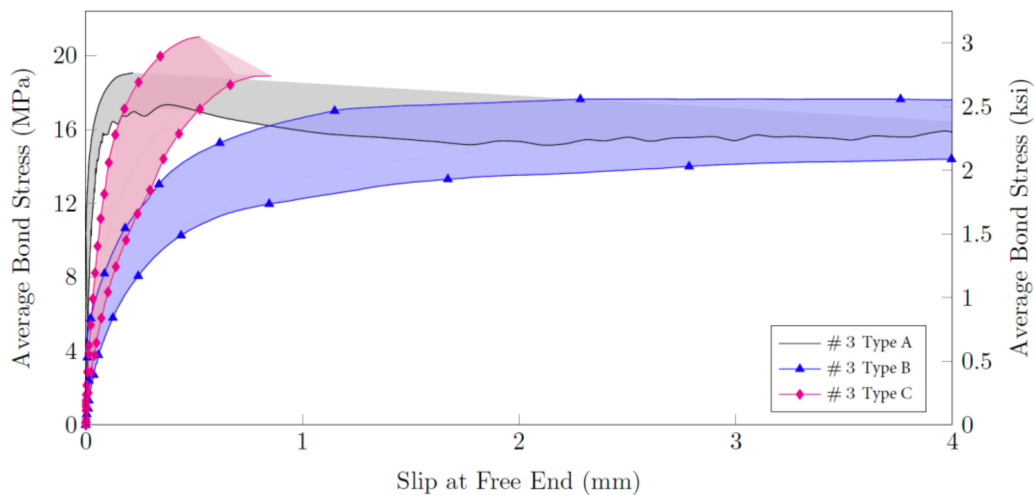
Figure 4. Bond-slip (free-end) behavior of unaged specimens.

It can be inferred that the bond-to-concrete behavior varied from rebar type to rebar type, as seen from the bond-slip graph in Figure 4; the initial slope, peak stress, slippage values and 'post-failure' behavior characteristics for each bar type. The ribbed rebars (type C) developed the highest maximum bond strength with a value of approximately 22.5 MPa; these were followed by the sand coated bars (type A) with about 18 MPa, while rebars with external cross fibers (type B) measured values ranging around 12.5 MPa. The peak bond strength for type A rebars was reached at a free-end slippage of about 0.25 mm, and after the peak, the bond strength decreased almost linearly. For rebars type B, the free-end slippage corresponding to the maximum bond strength, was about 20 times higher than the one for type A rebars (reaching approximately 5 mm). In this case, after the peak bond was reached, the bond strength decreased gradually. The 'post failure' behavior of type C rebars, however, was dissimilar to that of rebars type A and B: as soon as the maximum bond strength for the ribbed and sand coated rebars was attained (at about 0.7 mm), a sudden failure of the bond surface occurred.

After the bond behavior of the three GFRP rebar types was evaluated, the durability of this mechanical property was assessed on test specimens that were stored in seawater for different exposure times and temperatures. Accordingly, the potential fluctuation of the maximum bond strength over time was analyzed. Table 2 shows the average values of the "pull-out" peak load, as well as the average maximum bond strength values for the different bars and different exposure conditions.

For a better interpretation of the results, Figure 5 shows the evolution of the maximum bond strength values for the three types of bars exposed to 23, 40 and 60 °C. The bond of the Type-A bars after 60 days of exposure suffered a deterioration of around 10% in the case of the specimens exposed to seawater at 60 °C, and 18% at 23 °C, remaining unchanged at 40 °C. After 120 days, the three conditions converged to a deterioration of around 15%. The deterioration of Type-B rebars, however, remained effectively constant after 60 days of exposure at the three different temperatures. After 120 d, an increase in the bond capacity of around 15% was noted in the case of exposure at 23 and 40 °C, while the bond strength of the specimens exposed to 60 °C dropped by 5%. For Type-C rebars, after 60 days of exposure, showed a deterioration of 5% detected at 40 and 60 °C, compared to 10% in the case of exposure to 23 °C. After 120 days, on the contrary, a bond increase of 12% was noted for the rebars exposed to 23 °C, while those exposed to 40 and 60 °C suffered an additional 5% deterioration.
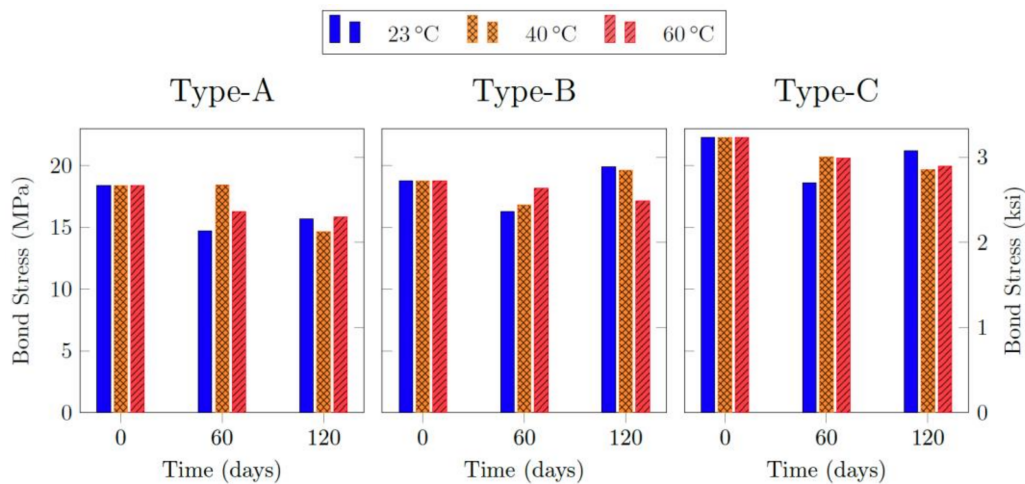
Figure 5. Bond strength development over time (rebar types A, B and C).

From the three graphs in Figure 5 corresponding to the evolution of the bond strength over time, it can be seen that the variation of this mechanical property was not significant after 120 days of exposure to seawater at 23, 40 or 60 °C; the values ranged between 10% and 15%, including cases with a bond strength increase. In addition, the effect of the temperature in accelerating the degradation did not seem to have caused a significant effect.

The graphs in Figure 6 facilitate a comparison between the three rebar types; it can be inferred that the type C rebar (with lugs) had the highest bond strength, whereas the type A (sand coated) and B rebars (helical grooved) had a similar mechanical bond. The bond deterioration was no more than 15% in all three cases after 120 days of exposure to seawater, regardless of the temperature.
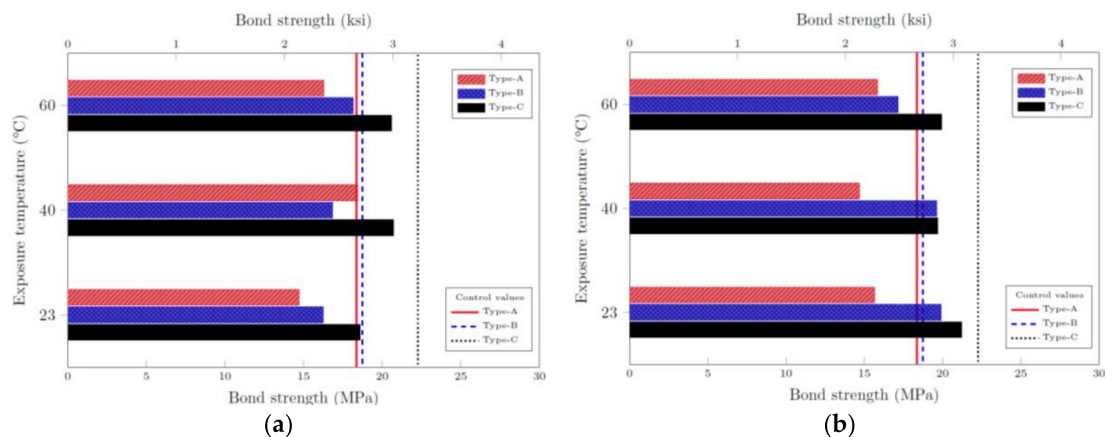

Figure 6. Bond strength development after 60 (**a**) and 120 days (**b**).

Failure Mechanisms

Every specimen tested showed a very similar failure mechanism: in all specimens (both control and conditioned), the failure occurred at the bond interface between the GFRP rebar and the concrete. No GFRP rebar failed in tension, nor was concrete splitting observed for any of the tested specimens, which differs from the observations made by others [11,20,21]. After the specimens were tested, the concrete blocks were split in half to evaluate the interface surface of the rebar (Figure 7).

Figure 7. Bond surface of the GFRP rebar after completion of the bond test: type A (**a**), type B (**b**) and type (**c**).

It can be seen that the damage to the rebars varied with the type of surface enhancement: for type A rebars, the sand coat was removed due to the friction between the rebar and the concrete. The type B rebars, however, showed damage in the most superficial fibers, though the helical groves were not completely lost. Finally, the lugs in the type C rebars were partially or completely cut off during the pullout test, but the internal glass fibers of the rebar were not exposed to the surface.

5. Conclusions

The durability of the bond between the GFRP rebars and concrete in coastal environments is a characteristic which, even though it is crucial, has not yet been fully evaluated. Considering the great importance of this mechanical property in the proper functioning of GFRP reinforced concrete structures, many institutions, such as the Florida Department of Transportation (FDOT), are directing efforts towards its evaluation. As part of these efforts, the bond mechanism of three different types of GFRP rebars (sand coated, helically grooved and with lugs) exposed to a marine environment was evaluated via 'pullout' tests.

The test results showed that GFRP rebars with different surface enhancements performed significantly differently to one another and showed dissimilar bond-slip behavior. Within the scope of the tested materials, the ribbed rebars (type C) offered the highest bond strength (22.5 MPa), followed by sand coated (type A) rebars (18 MPa), and rebars with external cross fibers (type B) (12.5 MPa).

The bond stress development was also affected based on the selected rebar type: sand coated rebars (type A) activate the full bond strength rapidly and exhibit the stiffest bond with concrete (free-end slippage). Type A rebars were followed by ribbed (type C) rebars, while the highest slippage may be expected for GFRP rebars with external cross fibers (type B); these rebars may slip about 20 times more than rebars with other surface enhancements. After the maximum bond was reached, type A and B rebars gradually debonded, while ribbed bars (type C) promoted a sudden-slip failure.

For the durability assessment of the bond strength, additional companion specimens were submerged in seawater tanks at different temperatures (23, 40 and 60 °C) for 60 and 120 days. The initial results showed that the deterioration of the bond strength may not be severe, though the specimens were tested under accelerated conditions. After 120 days of exposure in seawater at 23, 40 and 60 °C, the maximum bond strength varied around ±10% to 15%.

The bond failure mode of GFRP specimens in concrete depended on the surface enhancement and was independent of the exposure temperature or duration. All specimens failed at the interface between the surface enhancement and the concrete, but each bar type was damaged differently: type A rebars lost the sand coat and then slipped, type B rebars suffered partial damage of the longitudinal external fibers before slip-out, and finally, the lugs of the type C rebars were cut off but the glass fibers remained intact.

Further testing and a larger array of experiments under long-term exposure should be conducted to validate these initial finding or to provide additional data on the bond performance of GFRP reinforced concrete. Moreover, because bond deterioration was not observed for an exposure period

of 120 days, extended aging phases should be considered and evaluated for a better assessment of bond durability.

Author Contributions: Conceptualization, D.C.YB.F. and K.R.; Methodology, D.C.Y.B.F. and K.R.; Software, K.R.; Validation, R.E.A., K.R. and D.C.Y.B.F.; Formal Analysis, R.E.A., K.R. and D.C.Y.B.F.; Investigation, R.E.A., D.C.Y.B.F. and K.R.; Resources, D.C.Y.B.F. and K.R.; Data Curation, R.E.A., K.R. and D.C.Y.B.F.; Writing-Original Draft Preparation, R.E.A.; Writing-Review & Editing, R.E.A., K.R., D.C.Y.B.F. and A.U.I.; Visualization, R.E.A., R.K., D.C.Y.B.F. and A.U.I.; Supervision, R.E.A., K.R., D.C.Y.B.F. and A.U.I.; Project Administration, D.C.Y.B.F. and K.R.; Funding Acquisition, D.C.Y.B.F. and K.R.

Conflicts of Interest: The authors declare no conflict of interest. The funders had no role in the collection, analyses, or interpretation of data; in the writing of the manuscript, and in the decision to publish the results.

References

1. Ruiz Emparanza, A.; Kampmann, R.; y Basalo, F.D.C. State-of-the-Practice of Global Manufacturing of FRP Rebar and Specifications. In Proceedings of the ACI Fall Convention, Anaheim, CA, USA, 15–19 October 2017.
2. Robert, M.; Benmokrane, B. Combined effects of saline solution and moist concrete on long-term durability of GFRP reinforcing bars. *Constr. Build. Mater.* **2013**, *38*, 274–284. [CrossRef]
3. Micelli, F.; Nanni, A. Durability of FRP rods for concrete structures. *Constr. Build. Mater.* **2004**, *18*, 491–503. [CrossRef]
4. Gooranorimi, O.; Nanni, A. GFRP Reinforcement in Concrete after 15 Years of Service. *J. Compos. Constr.* **2017**, *21*, 04017024F. [CrossRef]
5. Chen, Y.; Davalos, J.F.; Ray, I.; Kim, H.Y. Accelerated aging tests for evaluations of durability performance of FRP reinforcing bars for concrete structures. *Compos. Struct.* **2007**, *78*, 101–111. [CrossRef]
6. Nanni, A.; Luca, A.D.; Zadeh, H.J. *Reinforced Concrete with FRP Bars: Mechanics and Design*; CRC Press: Boca Raton, FL, USA, 2014.
7. Kotynia, R.; Szczech, D.; Kaszubska, M. Bond Behavior of GRFP Bars to Concrete in Beam Test. *Procedia Eng.* **2017**, *193*, 401–408. [CrossRef]
8. ASTM International. *ASTM D7913—Standard Test Method for Bond Strength of Fiber-Reinforced Polymer Matrix Composite Bars to Concrete by Pullout Testing*; ASTM International: West Conshohocken, PA, USA, 2014.
9. Canadian Standards Association. *CSA S806-12—Design and Construction of Building Structures with Fibre-Reinforced Polymers*; Canadian Standards Association: Mississauga, ON, Canada, 2012.
10. Yan, F.; Lin, Z.; Yang, M. Bond mechanism and bond strength of GFRP bars to concrete: A review. *Compos. Part B Eng.* **2016**, *98*, 56–69. [CrossRef]
11. Altalmas, A.; El Refai, A.; Abed, F. Bond degradation of basalt fiber-reinforced polymer (BFRP) bars exposed to accelerated aging conditions. *Constr. Build. Mater.* **2015**, *81*, 162–171. [CrossRef]
12. Dong, Z.; Wu, G.; Xu, B.; Wang, X.; Taerwe, L. Bond durability of BFRP bars embedded in concrete under seawater conditions and the long-term bond strength prediction. *Mater. Des.* **2016**, *92*, 552–562. [CrossRef]
13. Robert, M.; Cousin, P.; Benmokrane, B. Durability of GFRP reinforcing bars embedded in moist concrete. *J. Compos. Constr.* **2009**, *13*, 66–73. [CrossRef]
14. Suraneni, P.; Jafari Azad, V.; Isgor, O.B.; Weiss, W.J. Deicing salts and durability of concrete pavement and joints. *Concr. Int.* **2016**, *38*, 48–54.
15. ASTM International. *ASTM C39—Standard Test Method for Compressive Strength of Cylindrical Concrete Specimens*; ASTM International: West Conshohocken, PA, USA, 2016. [CrossRef]
16. ASTM International. *ASTM D792—Standard Test Methods for Density and Specific Gravity (Relative Density) of Plastics by Displacement*; ASTM International: West Conshohocken, PA, USA, 2013.
17. ASTM International. *ASTM D7205—Standard Test Method for Tensile Properties of Fiber Reinforced Polymer Matrix Composite Bars*; ASTM International: West Conshohocken, PA, USA, 2011. [CrossRef]
18. Benmokrane, B.; Manalo, A.; Bouhet, J.; Mohamed, K.; Robert, M. Effects of Diameter on the Durability of Glass Fiber–Reinforced Polymer Bars Conditioned in Alkaline Solution. *J. Compos. Constr.* **2017**, *21*, 04017040. [CrossRef]

19.   ASTM International. *ASTM D7705—Standard Test Method for Alkali Resistance of Fiber Reinforced Polymer (FRP) Matrix Composite Bars Used in Concrete Construction*; ASTM International: West Conshohocken, PA, USA, 2012. [CrossRef]

20.   Gu, X.; Yu, B.; Wu, M. Experimental study of the bond performance and mechanical response of GFRP reinforced concrete. *Constr. Build. Mater.* **2016**, *114*, 407–415. [CrossRef]

21.   Okelo, R.; Yuan, R.L. Bond Strength of Fiber Reinforced Polymer Rebars in Normal Strength Concrete. *J. Compos. Constr.* **2005**, *9*, 203–213. [CrossRef]